

Solute Carrier Family 7 Member 11 (SLC7A11) is a Potential Prognostic Biomarker in Uterine Corpus Endometrial Carcinoma

Xiangming Fang^{1,*}, Ting Zhang^{2,*}, Zhitao Chen¹

¹Shulan (Hangzhou) Hospital Affiliated to Zhejiang Shuren University Shulan International Medical College, Hangzhou, People's Republic of China;

²Department of Pathology, Hangzhou Tongchuang Medical Laboratory, Hangzhou, People's Republic of China

*These authors contributed equally to this work

Correspondence: Xiangming Fang, Obstetrics and Gynecology Department, Shulan (Hangzhou) Hospital Affiliated to Zhejiang Shuren University Shulan International Medical College, 848# Dongxin Road, Hangzhou City, Zhejiang Province, 310000, People's Republic of China, Tel +86-0571-87236570, Email fxm1213@126.com

Background: Uterine corpus endometrial carcinoma (UCEC) is a common type of gynecological cancers, second only to cervical cancer in incidence. Thus, it is necessary to develop effective therapies and identify biomarkers for its prognosis. Solute carrier family 7 member 11 (SLC7A11) is well known for its role in maintaining the intracellular glutathione level and preventing oxidative-stress-induced cell death. However, the association between SLC7A11 expression and prognosis as well as the correlation between tumor-infiltrating immune cells (TIICs) and immunotherapy of UCEC has rarely been reported. This study aims to evaluate the prognostic significance and immune cell infiltration level of SLC7A11 in UCEC.

Methods: Bioinformatics analysis tools and databases, including R software, National Center for Biotechnology Information (NCBI), The Cancer Genome Atlas (TCGA), GEPIA2, Sangerbox, Kaplan–Meier (K-M) Plotter, TISIDB, and TIMER2, were utilized to measure the expression level and clarify the clinical significance of SLC7A11 in UCEC.

Results: SLC7A11 expression was dramatically up-regulated in UCEC patients and associated with prognosis. DNA methylation levels in the SLC7A11-promoter region were significantly higher in normal participants than in patients with UCEC. We also showed that SLC7A11 overexpression was associated with TIICs, immune checkpoint blockers (ICBs), and immunotherapy response in UCEC. The half-maximal inhibitory concentration (IC50) results obtained with the cohort from TCGA showed that Z-VAD-FMK (Caspase inhibitor), S-Triphenylmethyl-L-cysteine (S-Trityl-L-cysteine), and TAE684 (ALK inhibitor) had higher IC50 values in low-expression patient ($p < 0.05$).

Conclusion: SLC7A11 overexpression is associated with favorable prognosis of patients with UCEC and is associated with TIICs and the responses to immunotherapy.

Keywords: solute carrier family 7 member 11, uterine corpus endometrial carcinoma, prognosis, tumor-infiltrating immune cells, bioinformatics analysis

Introduction

Endometrial cancer (EC) is one of the most frequently diagnosed types of gynecological cancers, second only to cervical cancer in incidence.¹ More than 50,000 women die from EC worldwide each year.² Despite the development of diagnostic techniques and treatment means, the prognosis of advanced EC remains unsatisfactory.^{3,4} The therapeutic methods of EC mainly include surgery, radiotherapy, chemotherapy, and hormonal therapy.^{5,6} In the past decades, radical surgical resection and/or chemotherapy have been widely used for EC treatment.⁴ However, postoperative recurrence following radical resection is the main cause of early mortality of patients with EC.^{7,8} In the aspect of chemotherapy, although the first-line chemotherapeutic drugs for EC, namely, cisplatin and paclitaxel, can effectively inhibit cancer cell growth, their application is limited by the chemoresistance of cancer cells.⁹ In recent years, immunotherapy and targeted

therapy have been proved to be more effective and reliable EC treatment methods.^{10,11} Therefore, identifying new therapeutic targets, especially immune-related targets, to slow or even halt disease progression is an urgent priority.

Ferroptosis in tumor cells is described as a cell death mechanism involving the accumulation of iron-dependent reactive oxygen species (ROS).^{12,13} In recent years, ferroptosis has been found to be involved in the tumorigenesis of a variety of tumors.^{14,15} Solute carrier family 7 member 11 (SLC7A11) is well known for its role in maintaining intracellular glutathione levels and preventing oxidative-stress-induced cell death, such as ferroptosis. In addition, SLC7A11 is frequently over-expressed in cancers.¹⁶ It is the central regulator of ferroptosis, with its reduced expression level being the marker for ferroptosis.¹⁷ Various studies have shown that the SLC7A11 and SLC7A11-induced ferroptosis are involved in the tumorigenesis of human tumors, including colorectal cancer,¹⁸ gastric cancer,¹⁹ hepatocellular carcinoma,²⁰ and lung cancer.²¹ For example, Zhang et al²¹ uncovered a Uc.339/miR-339/SLC7A11 axis which leads to dysregulation in the ferroptosis in lung adenocarcinoma and constitutes an underlying mechanism that drives the tumorigenesis and metastasis of lung cancers. However, to our knowledge, the biological effects of SLC7A11 on EC have not been well understood.

In this study, through a bioinformatic study, we visualized the expression and prognostic value of SLC7A11 across EC and analyzed its association with immune cell infiltrates and immune biomarkers. In addition, we conducted a data mining to systematically explore whether SLC7A11 overexpression is associated with the response of patients with cancer to immunotherapy. Finally, we validated the expression level of tumor tissues from UCEC patients for SLC7A11 with immunohistochemistry staining.

Materials and Methods

Ethics Approval

This study conforms to the principles outlined in the Declaration of Helsinki, all the cases used in this study were approved by the Academic Committee of Shulan (Hangzhou) Hospital. Written informed consent was obtained from the study participants prior to the study commencement.

Multi-Omics Analysis of SLC7A11

In order to comprehensively understand the gene function, the multi-omics analysis of SLC7A11 was performed based on several databases. We first studied the chromosome localization of SLC7A11 in humans using the GeneCards database²² (<https://www.genecards.org/>). Then, we obtained the location of the conserved domain from the UniProt database²³ (<https://www.uniprot.org/>) and visualized it using Illustrator for Biological Sequences²⁴ (IBS, <http://ibs.biocuckoo.org/>) online service. Subsequently, the three-dimensional (3D) structures of SLC7A11 in UCSC were predicted by Genome Browser²⁵ (<http://genome.ucsc.edu/>). To further understand the biological role of SLC7A11, we confirmed the cellular locations of proteins in human cells based on the Human Protein Atlas²⁶ (HPA, <https://www.proteinatlas.org/>) database. In addition, the evolutionary conservation of amino acids in SLC7A11-encoded protein was estimated using the “HomoloGene” module of the National Center for Biotechnology Information (NCBI) (<https://www.ncbi.nlm.nih.gov/>). The mammalian phylogenetic tree was generated using the online tool in NCBI.

Expression Analysis and of SLC7A11

We first explored the mRNA expression levels of SLC7A11 in cancerous and noncancerous tissues using the “Gene_DE” module of TIMER2.0²⁷ (<http://timer.comp-genomics.org/>). The significance was explored by the Wilcoxon test, and the distribution of gene expression levels was displayed using box plots. The GEPIA2²⁸ (<http://gepia2.cancer-pku.cn>) database containing The Cancer Genome Atlas (TCGA) data and Genotype-Tissue Expression (GTEx, <https://www.gtexportal.org>) data of UCEC samples and normal samples was searched. The information obtained was utilized to compare the mRNA expressions of SLC7A11 in UCEC and paracancerous tissues. GSE17025²⁹ (Jul 09, 2009, USA, GPL570) dataset was obtained from the Gene Expression Omnibus (GEO, <http://www.ncbi.nlm.nih.gov/geo>) database for the validation of SLC7A11 expression results. “Limma” R package (R version 4.2.0, <https://www.rstudio.com/>) was used for differential expression analysis and $p < 0.05$ was regarded significant. In addition, a paired difference analysis of 19 samples was performed to compare SCL7A11 expression levels in EC tissues and paired paracancerous tissues.

Immunohistochemistry (IHC) and Quantitative Real-Time Polymerase Chain Reaction (qRT-PCR)

Thirty-five pairs of paraffin-embedded UCEC and corresponding paracancerous tissues were collected from Shulan (Hangzhou) Hospital. Four-micron slices were mounted onto charged slides and baked at 60°C for 2 h. Then, these four-micron sections were incubated with 1:200 dilution of SLC7A11/xCT Polyclonal antibody (Catalog number: 26864-1-AP, Proteintech). After incubation with the anti-rabbit secondary antibody for 1 h at room temperature, the result of antibody staining was shown by diaminobenzidine (DAB). Finally, the samples were dehydrated and mounted. All slices were visualized using the microscope (Nikon Eclipse E100, Nikon digital sight DS-U3, Japan). Total mRNA was isolated from transfected cells using Trizol reagent. Reverse transcriptase was used to convert RNA to cDNA (EasyScript® All-in-One First-Strand cDNA Synthesis SuperMix for qPCR, TransGen Biotech). mRNA expression levels were measured by qRT-PCR. Primer sequences are shown in [Table S1](#).

Prognostic Analysis of SLC7A11 in UCEC

To explore the potential prognostic value of SLC7A11, we analyzed the relationship between SLC7A11 expression and survival prognosis, including overall survival (OS) and disease-free survival (DFS) based on the Kaplan–Meier (K-M) curve outputted by Kaplan-Meier Plotter³⁰ (<http://kmplot.com/analysis/>). We also established a nomogram that integrated SLC7A11 expression values and other clinicopathological features to predict 1-, 3-, and 5-year OS rates of UCEC patients. The predictive performance of the nomogram was measured by receiver operating characteristic (ROC) curve via the “timeROC” R package. Furthermore, the calibration curves of 1-, 3-, and 5-year OS were plotted.

DNA Methylation Analysis of SLC7A11 in UCEC

We first compared the methylation levels of SLC7A11 in normal and tumor samples using UALCAN. We then obtained the relationship between the promoter methylation level of SLC7A11 and the tumor stage as well as pathologic classification. In addition, the correlation between SLC7A11 transcription expression, copy number and promoter methylation level in distinct cancer subtypes were computed via MEXPRESS³¹ (<https://mexpress.be/>) by Pearson correlation analysis. The MethSurv³² (<https://biit.cs.ut.ee/methsurv/>) was used to visualize SLC7A11 methylation and the correlation between SLC7A11 hyper/hypomethylation and OS obtained based on the K-M curve. Furthermore, a Spearman regression analysis based on the GSCA web-based analysis platform was conducted to assess the correlation between DNA methylation and miRNA expression.

Immune Cell, Immune Checkpoint, and Immunotherapeutic Response Analysis

In order to explore the degree of immune cell infiltration in subgroups characterized by different expression levels in the TCGA datasets, we calculated the enrichment scores of tumor-infiltrating immune cells (TIICs) in high-expression and low-expression subgroups using the CIBERSORT algorithm based on R. Furthermore, correlations between SLC7A11 expression and TIICs were assessed using lollipops and scatter plots. The relationship between the SLC7A11 expression and the profile of TIICs was also obtained from TIMER. Next, the TISIDB³³ (<http://cis.hku.hk/TISIDB/index.php>) website was searched to analyze the relationship between SLC7A11 and the abundance of immune checkpoint blockers (ICBs) molecules in UCEC. Statistically significant results ($p < 0.05$) were shown in scatter plots. In addition, the TIMER database was searched to validate the correlation between SLC7A11 and key ICBs, including PD-1, PD-L1, CTLA-4, and PD-L2.

SLC7A11 Expression and Drug Sensitivity

The relationships between the half-maximal inhibitory concentration (IC₅₀) of chemotherapeutic drugs and the SLC7A11 expression levels were investigated using the “pRRophetic” R package. With this algorithm, the IC₅₀ of different drugs was predicted for UCEC samples by searching the Genomics of Drug Sensitivity in Cancer (GDSC, www.cancerrxgene.org/). Furthermore, the chemical structural formula and molecular formula of significant chemotherapeutic drugs were explored.

Results

Multi-Omics Analysis of SLC7A11

This research project aims to evaluate the oncogenic role of SLC7A11 in UCEC. The SLC7A11 (Gene ID: 23657, updated on May 15, 2022) gene is located on chromosome 4q28.3 and contains 22 exons (Figure 1A). SLC7A11 (NM_014331.4) is induced by Nrf2 in human cancers. It encodes cystine/glutamate transporter (NP_055146.1) protein and contains one conserved domain (TIGR00911) (Figure 1A). The tertiary structure of SLC7A11-encoded protein was predicted based on the UCSC database (Figure 1B). In addition, the genomic regions, transcripts, and products were displayed (Figure S1A). We found that SLC7A11-encoded protein was mostly localized in the vesicles of human cells (Figure 1C), such as A-549 (human non-small cell lung cancer cells) and U-2 OS (human osteosarcoma cell line) (Figure 1D). Our finding has shown that the SLC7A11-encoded protein was highly conserved across species, such as

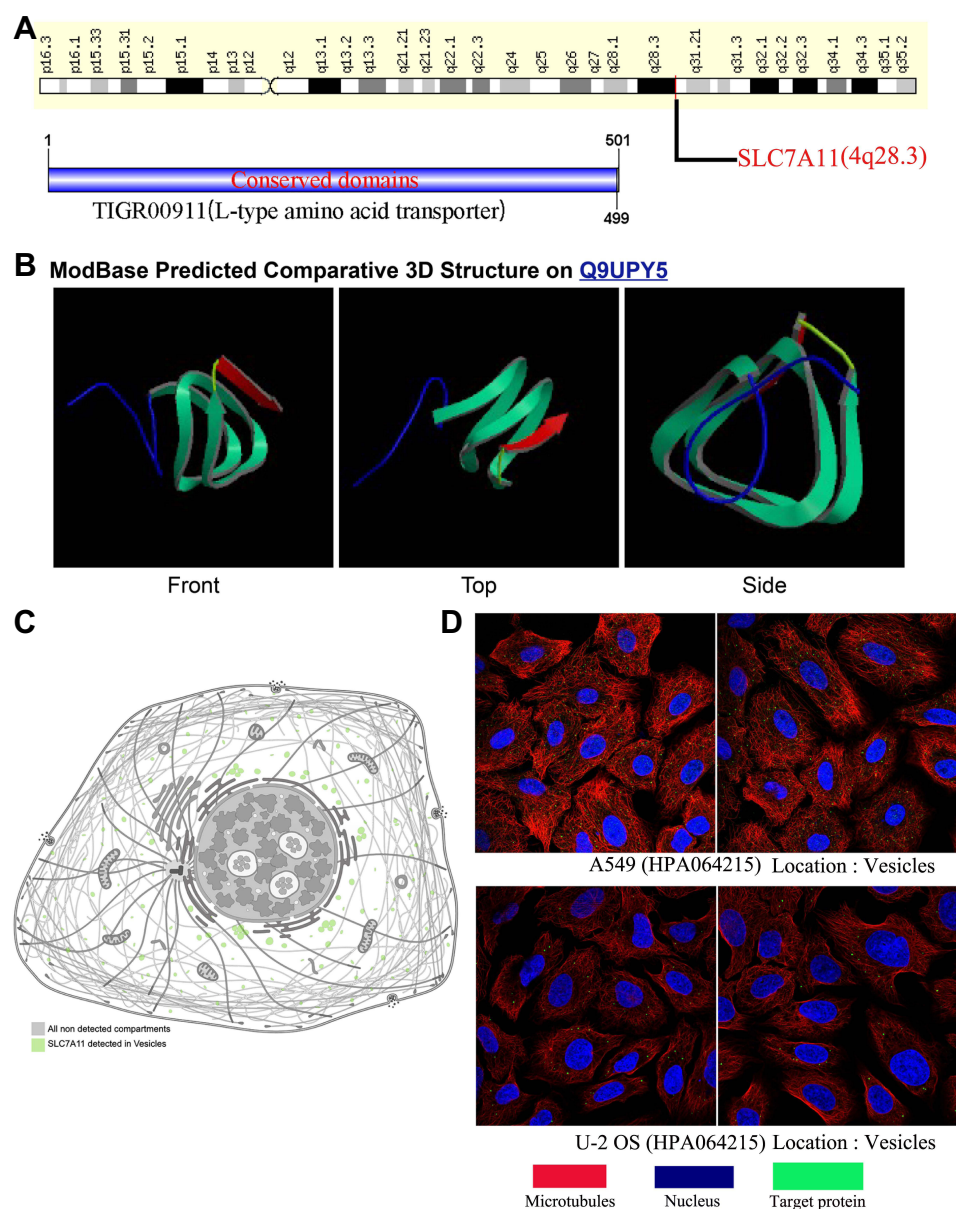


Figure 1 Chromosome localization, protein structure and protein localization analysis of Solute carrier family 7 member 11 (SLC7A11). **(A)** Chromosome localization and conserved domain of SLC7A11 in human. **(B)** The comparative three-dimensional (3D) structure of SLC7A11 protein. **(C)** The localization of SLC7A11 protein in human cells. **(D)** Analysis of SLC7A11 protein localization in A-549 (human non-small cell lung cancer cells) and U-2 OS (human osteosarcoma cells) cell lines.

Homo sapiens, *Pan troglodytes*, *Canis lupus familiaris*, *Macaca mulatta*, *Bos taurus*, *Rattus norvegicus* and *Mus musculus* (Figure S1B). The phylogenetic tree of SLC7A11-encoded protein was constructed and it presented the evolutionary relationship across species (Figure S1C). These results suggest a vital role of SLC7A11 in the biological function of eukaryotes.

Pan-Cancer Analysis of Expression of SLC7A11

We first analyzed the pattern of SLC7A11 expression in various tumors and normal tissues. As shown in Figure 2A, SLC7A11 expression levels were increased in various tumor tissues, including colon adenocarcinoma (COAD), breast invasive carcinoma (BRCA), kidney renal clear cell carcinoma (KIRC), esophageal carcinoma (ESCA), head and neck squamous cell carcinoma (HNSC), stomach adenocarcinoma (STAD), cholangiocarcinoma (CHOL), prostate adenocarcinoma (PRAD), kidney renal papillary cell carcinoma (KIRP), liver hepatocellular carcinoma (LIHC), lung adenocarcinoma (LUAD), kidney chromophobe (KICH), lung squamous cell carcinoma (LUSC), rectum adenocarcinoma (READ), and UCEC. These results indicate that SLC7A11 expression is associated with most tumor development.

Differential Expression Analysis of SLC7A11 in UCEC

We determined that SLC7A11 was more highly expressed in UCEC tissues than in paracancerous tissues (Figure 2A). This expression pattern was validated by GEPIA2, as shown in Figure 2B. The higher expression of SLC7A11 in UCEC tissues was also observed in different probes from the GSE17025 dataset (Figure 2C–E). R software analysis of SLC7A11 mRNA levels in cancer and para-cancerous tissues of the same UCEC patients from TCGA showed a consistent result that the SLC7A11 was up-regulated (Figure 2F). These results suggest that SLC7A11 is differentially expressed in UCEC and normal tissues and its expression may be associated with tumor progression. For further validation, the expression level of the SLC7A11 gene was analyzed by IHC. It was found that SLC7A11 mRNA is more highly expressed in tumor tissues than in normal tissues (Figure 3A–B). This result was further validated by qRT-PCR for 10 paired tumorous and adjacent tissue samples (Figure 3C). These results are similar to those that we have previously reported for different databases.

Prognostic Value of SLC7A11 in UCEC

Furthermore, the prognostic value of SLC7A11 was analyzed using the Kaplan–Meier plotter database. The hazard ratios and *p* values indicated that SLC7A11 was significantly associated with OS, with a higher expression representing better OS, but was not significantly associated with DFS (Figure 4A and B). The survival time in the upper quartile of the SLC7A11 high-expression cohort was 103.73 months, which was significantly higher than that of the low-expression cohort (37.57 months). These results show that a higher SLC7A11 expression level may predict a better prognosis in patients with UCEC. In order to determine potential prognostic indicators and predict prognosis for patients with UCEC, Cox proportional hazards regression analysis was performed to exclude confounder effects for 394 UCEC patients with effective survival information. It was found that the clinicopathological parameters, including age (≤ 65 Y and >65 Y) ($p = 6.7 \times 10^{-4}$, HR = 2.77, 95% CI 1.54–4.97), tumor stage (Stage I, Stage II, Stage III, and Stage IV) ($p = 2.6 \times 10^{-4}$, HR = 1.62, 95% CI 1.25–2.11), and tumor grade (G1, G2, and G3) ($p = 0.01$, HR = 1.80, 95% CI 1.14–2.84) were significantly associated with prognosis in UCEC (Table 1). We next established a nomogram that integrated SLC7A11 expression levels and clinicopathological features, including age, tumor grade and tumor stage, to predict the 1-, 3-, and 5-year OS (Figure 4C). Furthermore, the ROC analysis showed that the AUCs for 1-, 3-, and 5-year OS prediction were 0.84 (95% CI 0.96–0.7), 0.75 (95% CI 0.84–0.66), and 0.79 (95% CI 0.87–0.70), respectively (Figure 4D). The value obtained by the calibration curve for OS is in good agreement with the value predicted by the nomogram and the observed value (Figure 4E). These results validated the accuracy of the model in predicting OS in patients with UCEC.

DNA Methylation Analysis of SLC7A11 in UCEC

To determine whether DNA methylation affects the tumorigenesis and development of UCEC, we first compared methylation levels of SLC7A11 in tumor and paracancerous tissue. As shown in Figure 5A, DNA methylation levels in the SLC7A11-promoter region were significantly higher in normal participants than in patients with UCEC. In

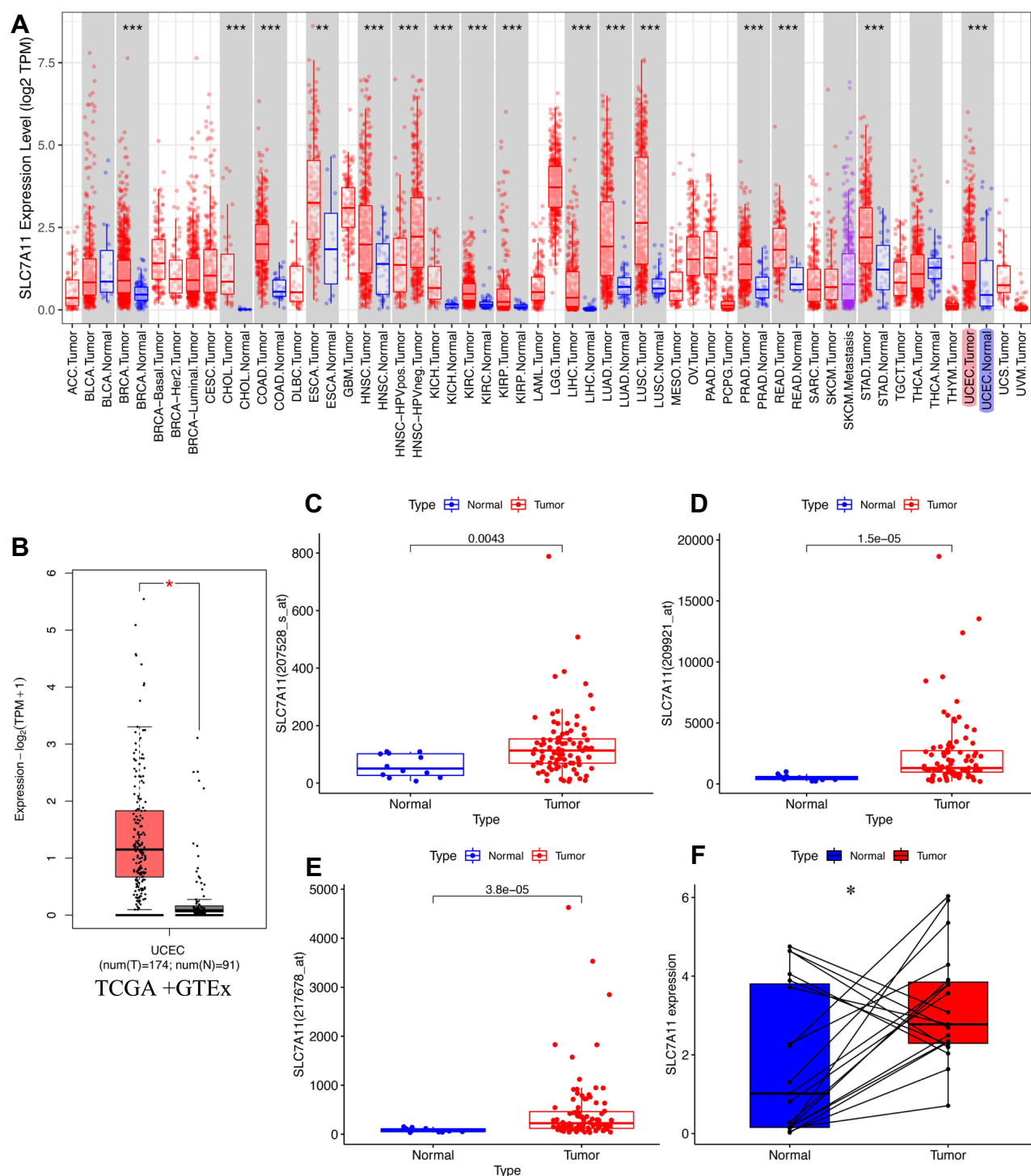


Figure 2 Expression analysis of Solute carrier family 7 member 11 (SLC7A11). **(A)** SLC7A11 expression level in tumor and normal tissues in The Cancer Genome Atlas (TCGA) pan-cancer data using TIMER. **(B)** Analysis using the GEPIA2 database showed that SLC7A11 had higher expression in Uterine corpus endometrial carcinoma (UCEC) compared to normal tissues. **(C-E)** The boxplots were used to compare the expression levels of SLC7A11 gene in the different probe, including **(C)** 207528-s-at, **(D)** 209921-at, and **(E)** 217678-at, of Gene Expression Omnibus (GEO) datasets. **(F)** Paired differential analysis of SLC7A11 in UCEC in the TCGA database. (* $p < 0.05$, ** $p < 0.01$, *** $p < 0.001$).

addition, we found that DNA methylation levels of SLC7A11 are higher at advanced tumor stages (stage 3 and stage 4) than at early tumor stages (stage 1 and stage 2) (Figure 5B). These results imply that the higher DNA methylation levels of SLC7A11 were correlated with the advanced tumor stage of patients with UCEC. DNA methylation levels of SLC7A11 were also detected in different types of UCEC, with the highest level observed in mixed serous and

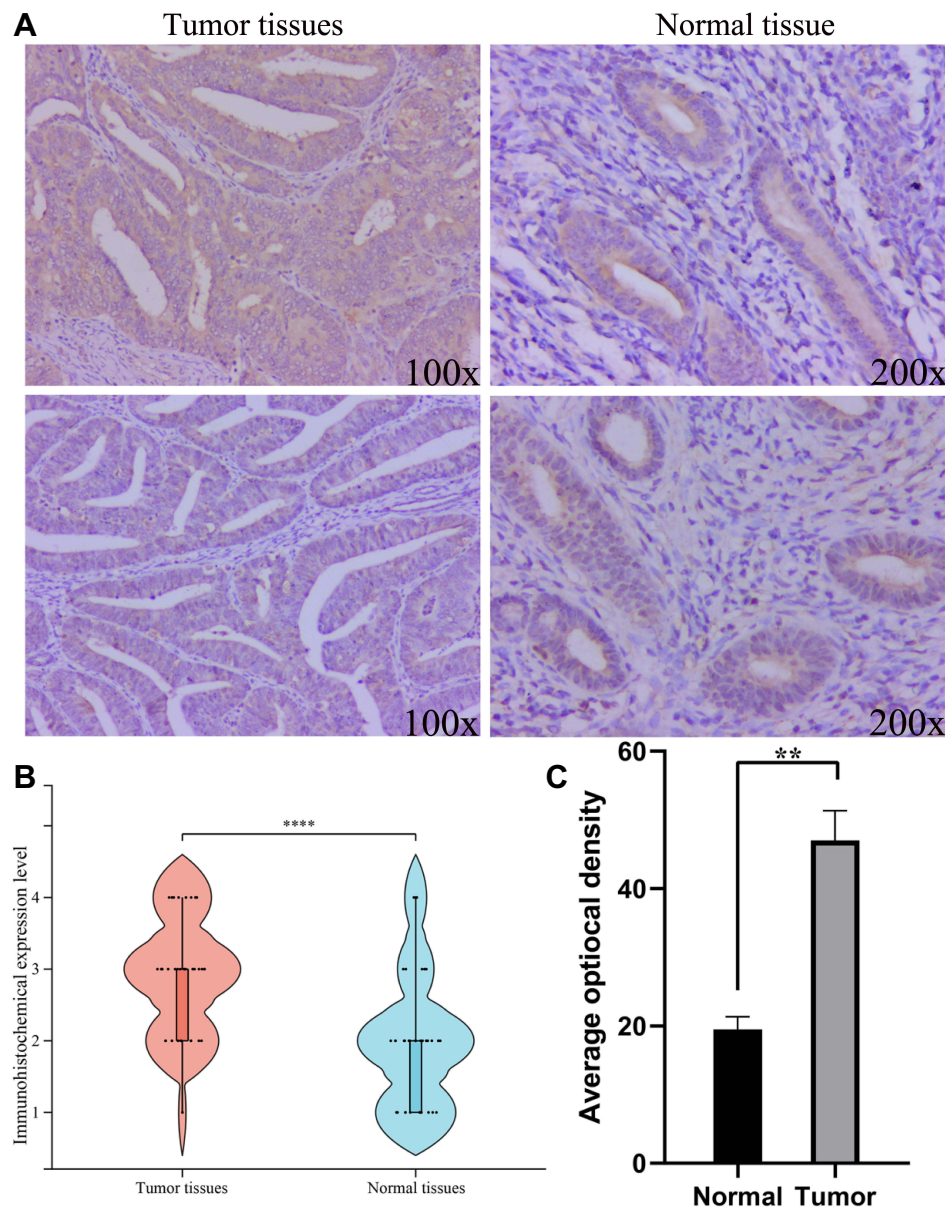


Figure 3 Solute carrier family 7 member 11 (SLC7A11) expression of Uterine corpus endometrial carcinoma (UCEC) tissue and the corresponding paracancerous tissue. **(A)** The expression level of SLC7A11 in UCEC and noncancerous tissues by immunohistochemistry. **(B)** SLC7A11 expression was high in 35 UCEC tissues than in the corresponding normal tissues by immunohistochemistry. **(C)** SLC7A11 expression was high in 10 UCEC tissues than in the corresponding normal tissues by quantitative real-time polymerase chain reaction (qRT-PCR).

endometrioid carcinoma, followed by the uterine serous carcinoma/uterine papillary serous carcinoma and uterine endometrioid carcinoma (Figure 5C). Additionally, the heat map of DNA methylation is displayed in Figure 5D. In cases from MEXPRESS, which were categorized based on clinical factors, including histological type, clinical stage and sample type, SLC7A11 displayed differences in expression patterns and copy number patterns (Figure S2A and S2B). We observed that five CpGs of SLC7A11 were significantly associated with the prognosis of UCEC (Figure 5E–I). The result also showed that SLC7A11 expression was significantly and inversely correlated with DNA methylation in the SLC7A11-promoter region (Figure 5J). Based on the MEXPRESS database, we also found that low promoter DNA methylation region was significantly associated with a high SLC7A11 expression status in most CpG islands (Figure S2C).

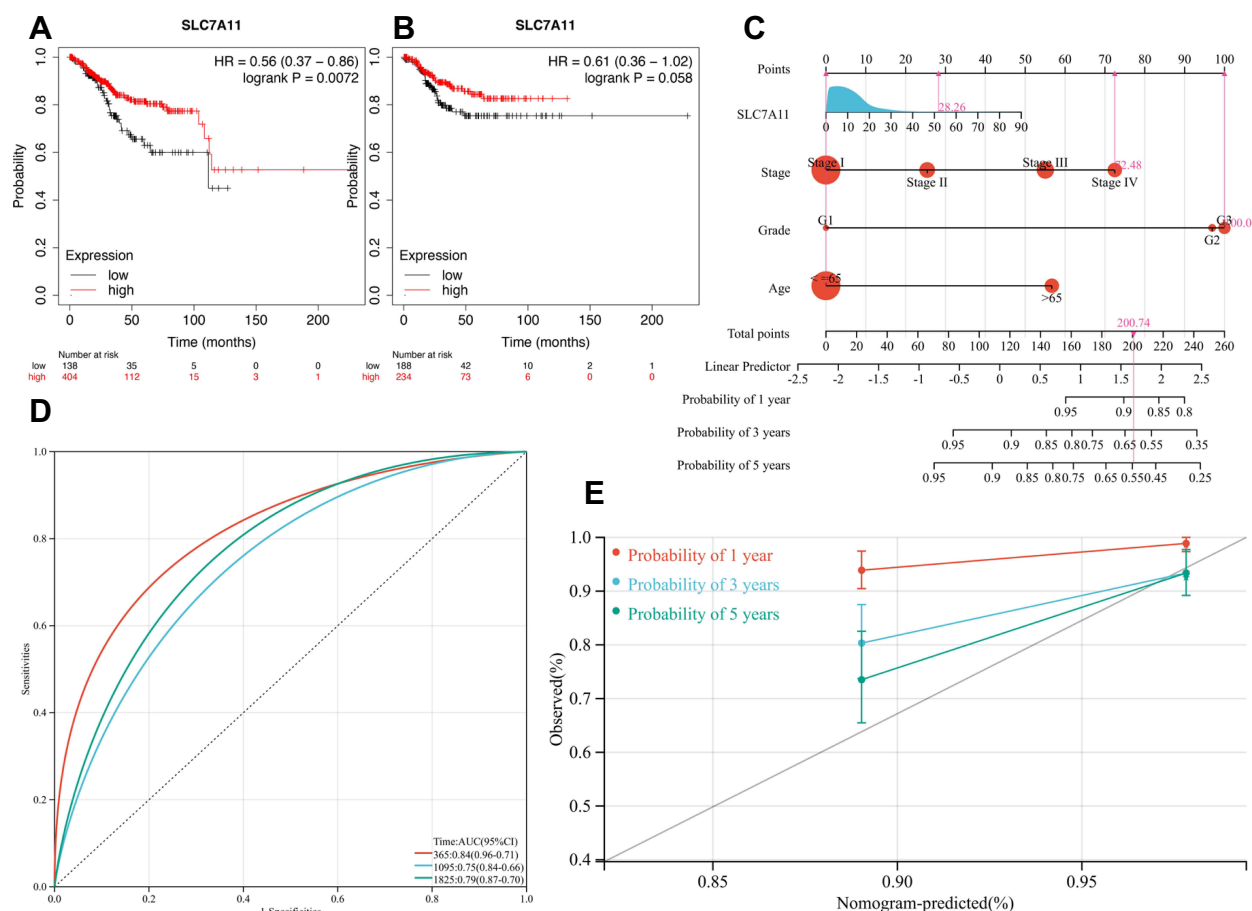


Figure 4 Predictive value of Solute carrier family 7 member 11 (SLC7A11) expression for clinical outcomes in Uterine corpus endometrial carcinoma (UCEC). (**A** and **B**) The Kaplan–Meier (K–M) curves of overall survival (OS) (**A**) and disease free survival (DFS) (**B**) shows the difference between the low- and high-expression of SLC7A11 in UCEC based on Kaplan–Meier Plotter database. (**C**) Composite nomogram prediction of 1-, 3-, and 5-year OS. (**D**) Time-dependent receiver operating characteristic (Td-ROC) curves for nomogram-mediated prediction of 1-, 3-, and 5-year OS in UCEC patients. (**E**) Calibration plot of the predictive nomogram.

Relationship Between SLC7A11 and Immune Cell Infiltration

The density of 22 tumor related immune cells from each sample was evaluated using CIBERSORT. It was found that naive B cells, memory B cells, activated CD4 memory T cells, gamma delta T cells, regulatory T cells (Tregs), and follicular helper T cells were the main immune cells affected by SLC7A11 expression (Figure 6A). Additionally, the expression of SLC7A11 was positively correlated with the infiltration level of activated CD4 memory T cells ($R = 0.19$, $p = 0.019$), follicular helper T cells ($R = 0.27$, $p = 6.0 \times 10^{-4}$), and gamma delta T cells ($R = 0.24$, $p = 0.0032$), but positively correlated with the infiltration level of Tregs ($R = -0.24$, $p = 0.0025$) (Figure 6B–F). We further explored the relationship between SLC7A11 expression level and TIICs in UCEC with the TIMER database. The results demonstrated that SLC7A11 expression level had positive correlations with several TIICs, including neutrophil ($\text{cor} = 0.178$, $p = 2.19 \times 10^{-3}$), CD4+ T cell ($\text{cor} = -0.154$, $p = 8.69 \times 10^{-3}$), CD8+ T cell

Table 1 The Cox Proportional Hazards Regression Analysis for Various Clinicopathological Parameters

Clinicopathological Parameters	HR	95% CI	p-value
Age (≤ 65 Y and > 65 Y)	2.77	1.54–4.97	6.70e-4
Stage (Stage I, Stage II, Stage III, and Stage IV)	1.62	1.25–2.11	2.60e-4
Grade (G1, G2, and G3)	1.80	1.14–2.84	0.01

Abbreviations: HR, hazard ratio; CI, confidence interval; Y, years; G, grade.

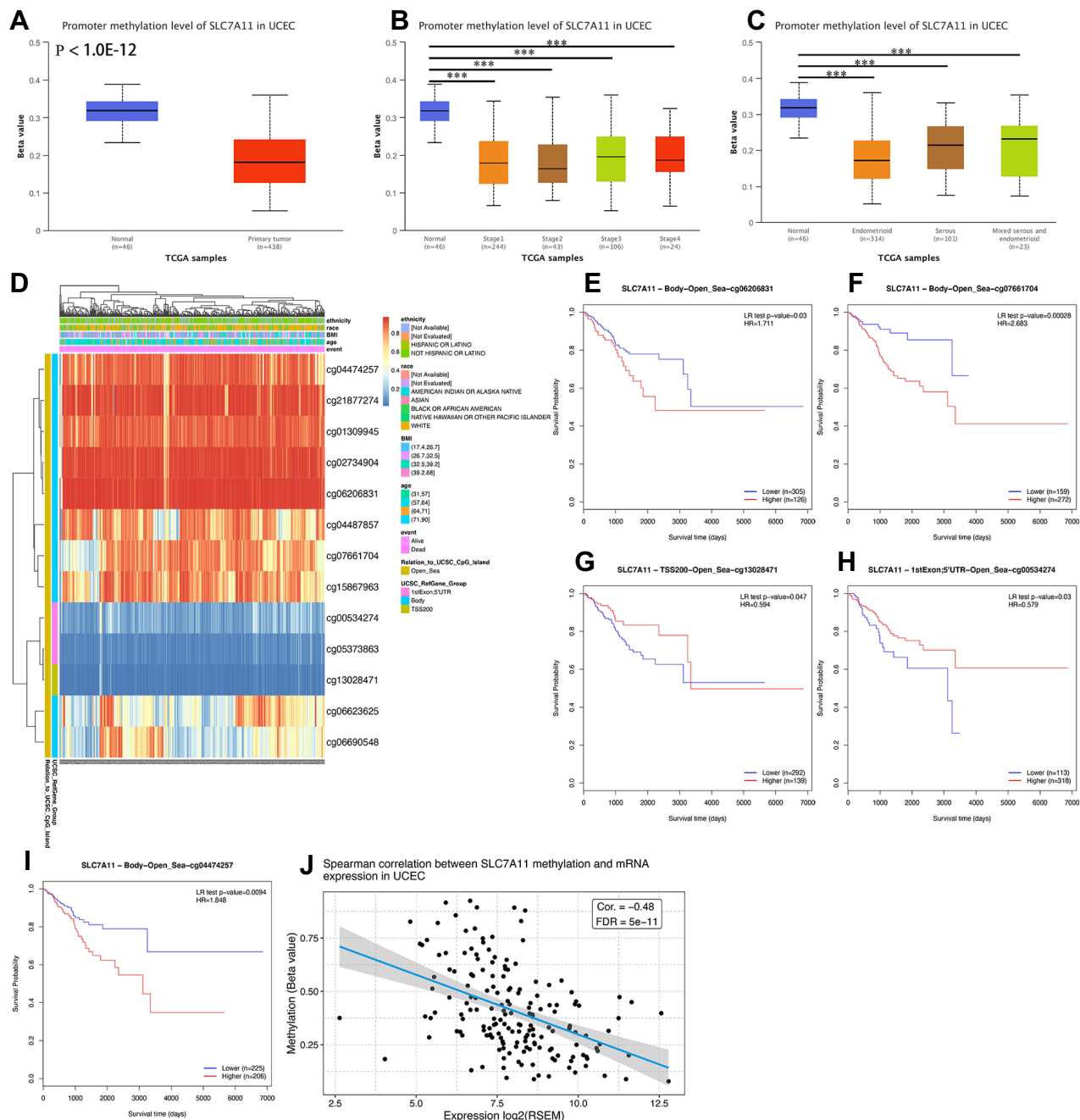


Figure 5 The DNA methylation analysis of Solute carrier family 7 member 11 (SLC7A11) in Uterine corpus endometrial carcinoma (UCEC). **(A)** Promoter methylation level of SLC7A11 in UCEC and normal tissues were analyzed with The Cancer Genome Atlas (TCGA) data by using UALCAN database. **(B)** Expression level of SLC7A11 methylation level in different TNM stages of UCEC. **(C)** Expression level of SLC7A11 methylation level in different pathological subtypes of UCEC. **(D)** The heat map showed the SLC7A11 DNA methylation at CpG sites. **(E-I)** the Kaplan-Meier **(K-M)** curves of overall survival (OS) shows the difference between the low- and high-expression of SLC7A11 methylation of cg06206831 **(E)**, cg07661704 **(F)**, cg13028471 **(G)**, cg00534274 **(H)**, and cg04474257 **(I)** CpG sites in UCEC. **(J)** Correlation between SLC7A11 mRNA expression and DNA methylation level was analyzed.

($\text{cor} = 0.325$, $p = 1.57\text{e-}08$) and dendritic cell ($\text{cor} = 0.235$, $p = 4.98\text{e-}05$) (Figure 6G). Many of chemokines are important for the regulation of chemotaxis of immune cells, especially T lymphocyte, monocytes/macrophages, and eosinophils.³⁴ As listed in Table 2, SLC7A11 expression was significantly positively correlated with T lymphocyte-related chemokines and monocyte/macrophage-related chemokines (CCL22), mast cell-related chemokines (CCR3 and CXCR4), eosinophil-related chemokines (CCL24) in UCEC. These findings indicate that SLC7A11 expression may regulate immune cell infiltration in UCEC.

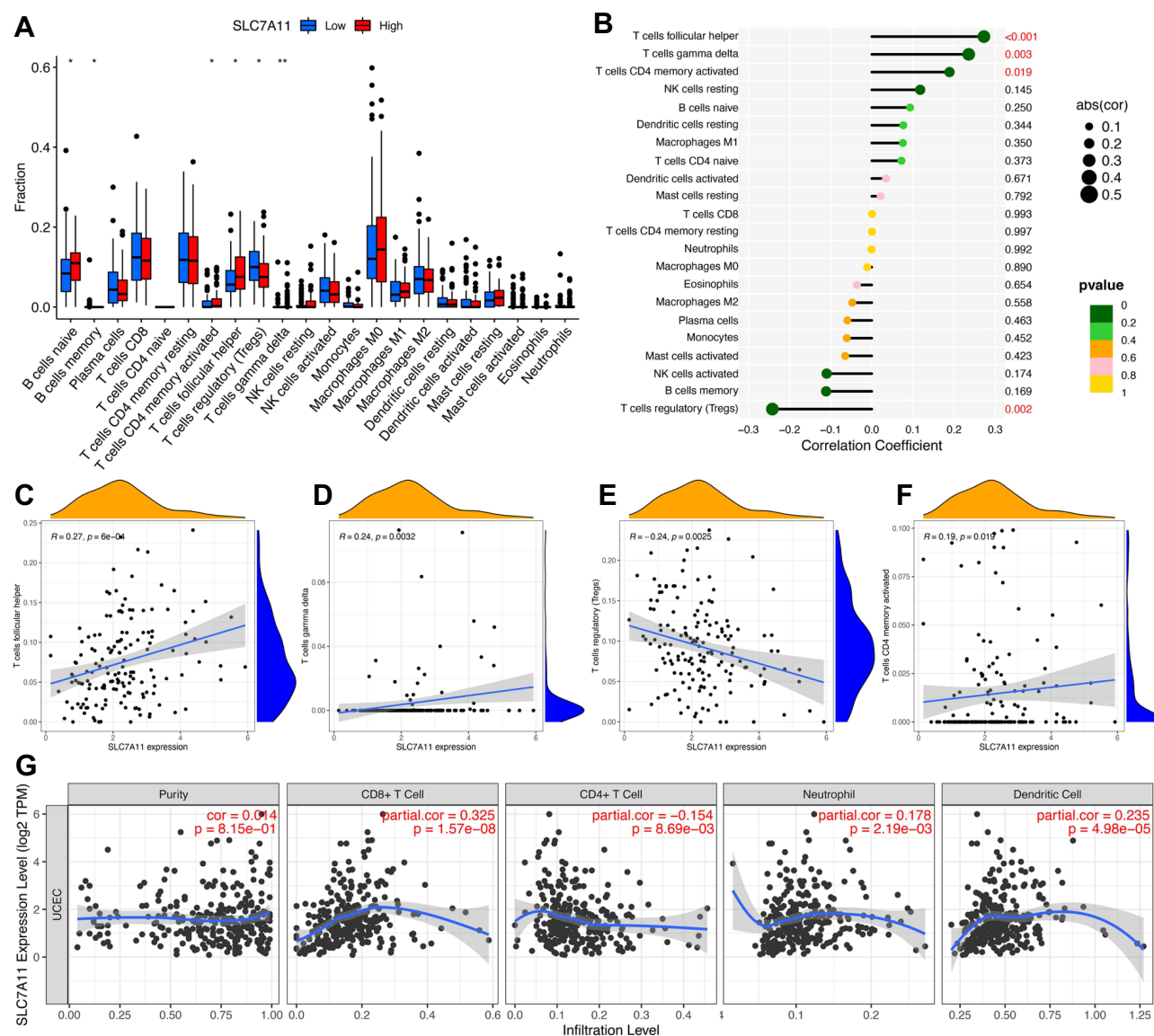


Figure 6 Correlation of Solute carrier family 7 member 11 (SLC7A11) expression with immune cells infiltration level in Uterine corpus endometrial carcinoma (UCEC). (A) Comparison of the enrichment scores of 22 types of immune cells between in high-SLC7A11 expression subgroup and low-SLC7A11 expression subgroup in the The Cancer Genome Atlas (TCGA) cohort. (B) The correlation between the SLC7A11 expression and immune cells. (C-F) The significant correlation between the SLC7A11 expression and immune cells including T cells follicular helper (C), T cells gamma delta (D), T cells regulatory (Tregs) (E), and T cells CD4 memory activated (F) in UCEC. (G) The correlation between the SLC7A11 expression and immune cells was conducted in the TIMER database and evaluated by Spearman correlation.

SLC7A11 Expression Was Correlated with Immune Checkpoint Molecules

We selected some important immune molecules, which have been verified to be associated with the efficacy of ICBs, to explore the associations between SLC7A11 expression and immune checkpoint molecules (Figure 7A). SLC7A11 expression was positively correlated with immunostimulators, including TGFBR1 ($\rho = 0.271$, $p = 1.50 \times 10^{-10}$), CD274 ($\rho = 0.148$, $p = 5.36 \times 10^{-4}$), CTLA4 ($\rho = 0.189$, $p = 0.55 \times 10^{-6}$), IDO1 ($\rho = 0.148$, $p = 5.27 \times 10^{-4}$), IL10 ($\rho = 0.218$, $p = 2.87 \times 10^{-7}$), KDR ($\rho = 0.197$, $p = 3.75 \times 10^{-6}$), PDCD1 ($\rho = 0.111$, $p = 9.71 \times 10^{-3}$), PDCD1LG2 ($\rho = 0.111$, $p = 9.74 \times 10^{-3}$), and TIGIT ($\rho = 0.087$, $p = 0.043$) in UCEC (Figure 7B–J). Furthermore, the expression of SLC7A11 was significantly negatively correlated with the following ICBs: CD160 ($\rho = -0.182$, $p = 2.05 \times 10^{-5}$), PVRL2 ($\rho = -0.286$, $p = 1.27 \times 10^{-11}$), and VTCN1 ($\rho = -0.153$, $p = 3.30 \times 10^{-4}$) in UCEC (Figure 7K–M). Considering the importance of the PD-1 (PDCD1), PD-L1 (CD274), PD-L2 (PDCD1LG2), and CTLA-4 to immune escape and immunotherapy, we analyzed the correlation between SLC7A11 expression and these ICBs based on the GEPIA2 database. The results

Table 2 The Correlation Between SLC7A11 Expression and Chemotactic Activity for Immune Cells in UCEC

Immune Cells	Chemokine	Cor	P-value
Monocytes/macrophages	CCL2	-0.063	4.10E-01
	CCL3	-0.054	4.80E-01
	CCL5	-0.066	3.80E-01
	CCL7	0.015	8.40E-01
	CCL8	-0.051	5.00E-01
	CCL13	0.035	6.50E-01
	CCL17	-0.045	5.50E-01
	CCL22	0.22	3.30E-03
T lymphocyte	CCL2	-0.063	4.10E-01
	CCL1	-0.043	5.70E-01
	CCL22	0.22	3.30E-03
Mast cells	CCL17	-0.045	5.50E-01
	CCR1	0.093	2.20E-01
	CCR2	0.038	6.20E-01
	CCR3	0.2	9.60E-03
	CCR4	0.061	4.30E-01
	CCR5	0.072	3.50E-01
	CXCR2	0.027	7.20E-01
Eosinophils	CXCR4	0.53	5.60e-14
	CCL11	0.0082	9.10E-01
	CCL24	0.29	9.90e-05
	CCL26	0.083	2.80E-01
	CCL5	-0.066	3.80E-01
	CCL7	0.015	8.40E-01
	CCL13	0.035	6.50E-01
Neutrophils	CCL3	-0.054	4.80E-01
	CXCL8	0.054	4.80E-01

Note: P value less than 0.05 is shown in bold.

Abbreviations: SLC7A11, Solute carrier family 7 member 11; CXCL, C-X-C motif chemokine ligand; CCL, C-C motif chemokine ligand; CXCR, C-X-C motif chemokine receptor; CCR, C-C motif chemokine receptor; UCEC, Uterine corpus endometrial carcinoma.

further confirmed that SLC7A11 expression is significantly associated with PD-1 (cor = 0.119, $p = 5.60 \times 10^{-3}$, [Figure 7O](#)), PD-L1 (cor = 0.251, $p = 2.73 \times 10^{-9}$, [Figure 7P](#)), PD-L2 (cor = 0.169, $p = 7.42 \times 10^{-5}$, [Figure 7Q](#)), and CTLA-4 (cor = 0.192, $p = 6.46 \times 10^{-6}$, [Figure 7R](#)) in UCEC. These results showed that SLC7A11 expression was increased in UCEC tumor tissues and implied that the upregulation of SLC7A11 in UCEC might play a considerable role in tumor immunotherapy.

SLC7A11 Expression and Drug Sensitivity

The IC₅₀ values of four common chemotherapy drugs were predicted in different SLC7A11 expression subgroups. The results obtained with the cohort from TCGA showed that Z-VAD-FMK (Caspase inhibitor), S-Triphenylmethyl-L-cysteine (S-Trityl-L-cysteine), and TAE684 (ALK inhibitor) had higher IC₅₀ values in low-expression patients, indicating that high-expression patients could be more sensitive to these chemotherapy drugs ([Figure 8A–C](#)). However, salubrinal had higher IC₅₀ values in high-expression patients, indicating that low-expression patients could be more sensitive to this chemotherapy drug ([Figure 8D](#)). The chemical structural formula and molecular formula of these chemotherapy drugs were displayed ([Figure 8E–H](#)).

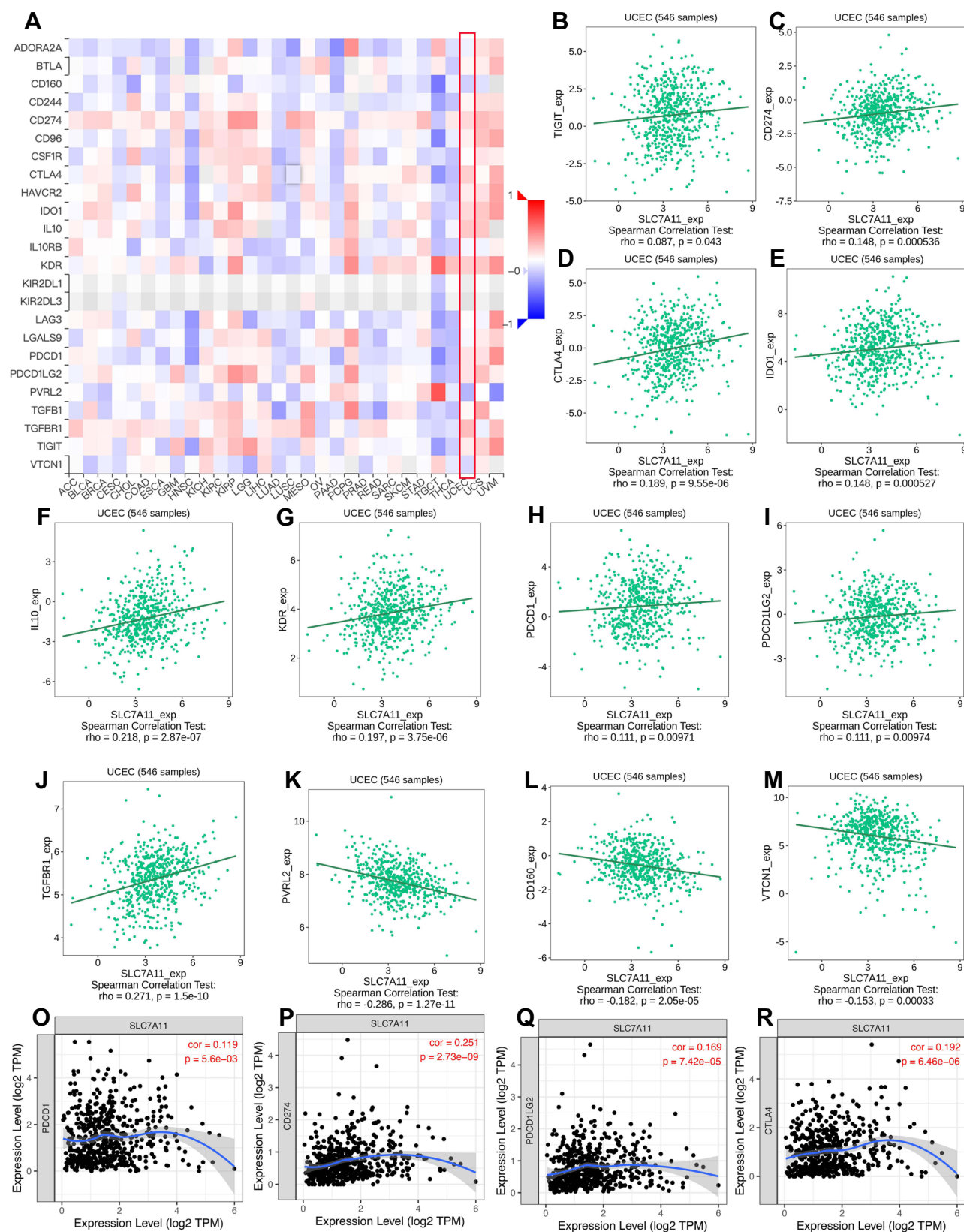


Figure 7 The Correlation between Solute carrier family 7 member 11 (SLC7A11) expression and immune checkpoint blockers (ICBs) in TISIDB and TIMER. **(A)** The panoramic association between the SLC7A11 expression and ICBs (red represents the positive correlation, and blue represents the negative correlation). **(B-M)** The significant association between the SLC7A11 expression and most ICBs, including TIGIT **(B)**, CD274 **(C)**, CTLA4 **(D)**, IDO1 **(E)**, IL10 **(F)**, KDR **(G)**, PDCD1 **(H)**, PDCD1LG2 **(I)**, TGFBR1 **(J)**, PVRL2 **(K)**, CD160 **(L)**, and VTCN1 **(M)**, in UCEC using TISIDB. **(O-Q)** The significant association between the SLC7A11 expression and most ICBs, including PDCD1 **(O)**, CD274 **(P)**, PDCD1LG2 **(Q)**, CTLA4 **(R)**, in UCEC using TIMER.

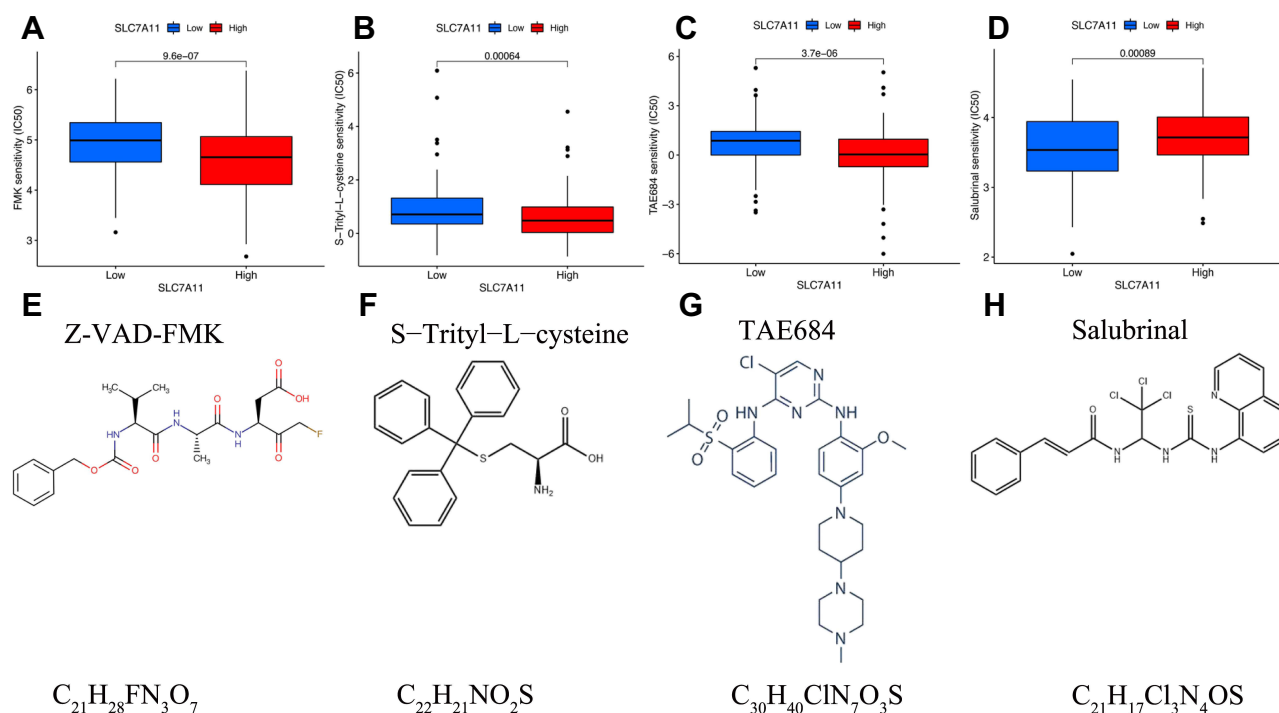


Figure 8 The significance of the Solute carrier family 7 member 11 (SLC7A11) expression in chemosensitivity. (A–D) Sensitivity performance of common chemotherapy agents, including Z-VAD-FMK (A), S-Triphenylmethyl-L-cysteine (S-Trityl-L-cysteine) (B), TAE684 (C), and Salubrinal (D), in high-SLC7A11 expression subgroup and low-SLC7A11 expression subgroup. (E–H) The chemical structural formula and molecular formula of these chemotherapy drugs; Z-VAD-FMK (A), S-Trityl-L-cysteine (B), TAE684 (C), and Salubrinal (D).

Discussion

EC, that is UCEC, ranks fourth in the incidence rate among the most common cancers in women in industrialized countries.³⁵ Approximately 280000 EC cases are reported worldwide every year.^{1,36} EC is tightly associated with unopposed estrogen exposure, endometrial hyperplasia, and genetic alterations.³⁷ With the development of whole-exome sequencing (WES) and whole-genome sequencing (WGS), it is becoming increasingly clear that tumorigenesis is attributed to genetic mutation and developmental context.^{38,39} Tumor occurrence and development mainly depend on the activation of proto-oncogenes and the inactivation of tumor suppressor genes. In addition, the compromise of gene expression patterns results in genomic instability, altered gene expression patterns and tumor formation.⁴⁰ The investigation of the molecular basis of cancer and the discovery of cancer-associated oncogenes in the 1980s have made cancer become treatable.⁴¹ Increasing studies indicate that SLC7A11 plays a significant role in the tumorigenesis and tumor progression by regulating tumor-associated oncogenes through interacting with different proteins.^{18,42} Nevertheless, the precise biological role and underlying mechanisms of SLC7A11 in EC remain indistinct.

Studies show that ferroptosis is a novel type of programmed cell death, which can effectively inhibit tumor cell growth, and it plays a significant role in tumorigenesis and tumor progression.^{13,43,44} SLC7A11 has a well-established role in maintaining intracellular glutathione levels and preventing oxidative-stress-induced cell death, such as ferroptosis,^{17,43,45,46} and SLC7A11 is frequently overexpressed in cancers.^{16,18,47,48} In addition, SLC7A11 imports extracellular cystine into cells to promote glutathione synthesis, thus inhibiting ferroptosis.⁴⁹ It was reported that ferroptosis was closely related to several endometrial diseases, such as endometriosis,^{50,51} repeated implantation failure,⁵² and endometrial hyperplasia,⁵³ and it can act as a therapeutic target for these diseases. Notably, the abnormal biological behaviors of EC patients are tightly associated with the occurrence of adenomyosis and endometriosis. Hence, it is necessary to investigate the biological role of SLC7A11 in EC development. Therefore, we performed a bioinformatics analysis to systematically explore whether the abnormal expression of SLC7A11 is associated with the clinical prognosis and tumorigenesis of EC patients and their response to immunotherapies.

In the present study, we found that SLC7A11 expression was significantly higher in UCEC tissues than in paracancerous tissues, and its methylation level had a significant positive correlation with UCEC pathological stage and pathological classification. We also found that a high SLC7A11 methylation level predicted an advanced clinical

pTNM stage in UCEC patients. It is well known that pTNM stage is a dependent predictor for the prediction of clinical outcomes of UCEC patients and is strongly associated with tumor recurrence or distant metastasis.⁵⁴ Our results showed that abnormal SLC7A11 methylation may play a functional role in tumor recurrence and distant metastasis in UCEC patients. However, UCEC patients with higher SLC7A11 transcript levels had significantly longer OS. It was proved again that SLC7A11 transcript levels were negatively associated with the degree of methylation. These findings suggest that SLC7A11 has a key role in the progression of UCEC. We further discovered that abnormal expression level of SLC7A11 was significantly associated with the infiltration levels of immune cells and cancer immunotherapy in UCEC.

Additionally, we also found that the SLC7A11 gene encodes a member of a heteromeric and sodium-independent anionic amino acid transport system that is highly specific to cysteine and glutamate based on the gene annotation from NCBI. SLC7A11 protein is an important cystine/glutamate transporter that is highly conserved across eukaryotes.⁴⁹ Furthermore, the SLC7A11 protein possesses the most conserved region (TIGR00911) of the human solute carrier (SLC) family proteins, which plays an important role in the transportation and binding of proteins, amino acids, peptides and amines. Our findings also revealed that the SLC7A11 protein was localized in the vesicles of human cells. These biological characteristics are essential for the development and function of human cells.

Neoplasms may harbor mutations in genes classically found in tumors originating from different tissues.⁵⁵ During cancer progression, genetic mutations can alter protein expression levels and then affect tumor growth and metastasis. By pan-cancer identification of genetic alterations of SLC7A11, Lin et al⁴⁸ has found that the mutation rate of SLC7A11 was less than 8% and that the main mutation type was missense mutation in human cancers. It is worth noting that missense mutation occurred most frequently in patients with EC.⁴⁸ More importantly, in the present study, we found that patients with EC whose tumor cells lost SLC7A11 expression due to gene mutation had a shortened survival rate than those whose tumor cells did not have SLC7A11 gene mutation. This result indicates that SLC7A11 expression may inhibit tumor progression in EC.

Several studies have shown that changes in DNA methylation patterns are associated with the development and progression of tumors.⁵⁶ In the present study, we found that DNA methylation levels in the SLC7A11-promoter region were significantly higher in normal participants than in patients with UCEC. And DNA methylation levels of SLC7A11 are higher at advanced tumor stages than at early tumor stages. So, we suggested that DNA methylation is another effective epigenetic mechanism involved in UCEC progression. Additionally, methylation of SLC7A11 CpG islands also increases in malignant tissues and contributes to tumorigenesis.

Recently, immune cell and stromal cell infiltration in TME was widely studied, which provided a novel potential approach for cancer treatment.⁵⁷ Immune cell infiltration contributes to immunosurveillance, eliminates tumor cells and slows immune evasion. A multitude of studies have also suggested that patients with immunological (or T-cell-infiltrated) tumors responded better to immune checkpoint inhibition than patients with non-immunological (or non-T-cell-infiltrated) tumors.⁵⁸ Additionally, immune cell infiltration has been found to be closely implicated in the clinical outcome.⁵⁹ TILs have also been found to be independent predictors of cancer survival.⁶⁰ Our findings showed that the abnormal expression level of SLC7A11 was significantly associated especially with the infiltration levels of lymphocytes, neutrophils, and dendritic cells in UCEC. TILs play a crucial role in antitumor immunity. PD-L1 was detected in tumor cells as well as intraepithelial TILs and stromal TILs. It can be summarized that SLC7A11 expression may affect the prognosis by affecting the infiltration of tumor-related immune cells. Cancer immunotherapy has greatly advanced in recent years, and the introduction of PD-1/PD-L1 blocking therapy has become a major pillar of immunotherapy.⁶¹ Immunotherapeutic strategies, including targeting specific ICBs as well as directing T cells toward diseased cells, are being applied for the treatment of several malignancies, including gynecological cancers.⁶² Immunotherapy is an active area of cancer research, especially the immune checkpoint PD-1/PD-L1-based immunotherapy.⁶⁰ We found that the SLC7A11 expression was not only associated with TIICs but also correlated with the expression of ICBs. The appropriateness of the treatment via ICBs can be assessed by the evaluation of the SLC7A11 expression in UCEC. It could also be speculated that the antitumor effect of immune cells may be affected by ICB pathways, given that SLC7A11 expression was correlated with the expression of ICB targets. We also found that SLC7A11 expression was significantly associated with inflammatory factors, numerous immune checkpoint markers, and immune activation pathways. Higher SLC7A11 expression is correlated with a higher survival rate, higher lymphocyte infiltration level and higher expression level of ICB-related genes. This finding may offer an insight into the therapeutics of UCEC.

Conclusions

The SLC7A11 expression was higher in UCEC than in normal tissues, and the high expression was associated with a favorable prognosis in UCEC patients. The expression status of SLC7A11 is not only related to immune cell infiltration but also the effectiveness of immunotherapies.

Abbreviations

SLC7A11, Solute carrier family 7 member 11; TIICs, tumor-infiltrating immune cells; EC, Endometrial cancer; ROS, reactive oxygen species; IBS, Illustrator for biological sequences; 3D, three-dimensional; IC50, half-maximal inhibitory concentration; GDSC, Genomics of Drug Sensitivity in Cancer; HRs, hazard ratios; ncRNAs, non-coding RNA; TCGA, The Cancer Genome Atlas; GTEx, Genotype-Tissue Expression; BRCA, breast invasive carcinoma; CHOL, cholangiocarcinoma; COAD, colon adenocarcinoma; ESCA, esophageal carcinoma; HNSC, head and neck squamous cell carcinoma; KICH, kidney chromophobe; KIRC, kidney renal clear cell carcinoma; KIRP, kidney renal papillary cell carcinoma; LIHC, liver hepatocellular carcinoma; LUAD, lung adenocarcinoma; LUSC, lung squamous cell carcinoma; PRAD, prostate adenocarcinoma; READ, rectum adenocarcinoma; STAD, stomach adenocarcinoma; UCEC, uterine corpus endometrial carcinoma; NCBI, National Center for Biotechnology Information; HPA, Human Protein Atlas; FC, Fold change; OS, overall survival; DFS, disease-free survival; K-M, Kaplan-Meier; TME, tumor microenvironment; ICIs immune checkpoint inhibitors.

Data Sharing Statement

The datasets used and analyzed in the present study are available from the corresponding authors on reasonable request. The datasets generated and/or analyzed during the current study are available in TCGA (<https://portal.gdc.cancer.gov>) and GEO (<https://www.ncbi.nlm.nih.gov/geo/>) databases.

Ethics Approval and Consent to Participate

This study conforms to the principles outlined in the Declaration of Helsinki (World Medical Association Declaration of Helsinki), all the cases used in this study were approved by the Academic Committee of Shulan (Hangzhou) Hospital. Written informed consent was obtained from the study participants prior to the study commencement.

Acknowledgments

The authors acknowledge the support of the open-access resources.

Author Contributions

All authors made substantial contributions to conception and design, acquisition of data, or analysis and interpretation of data; took part in drafting the article or revising it critically for important intellectual content; agreed to submit to the current journal; gave final approval of the version to be published; and agreed to be accountable for all aspects of the work.

Funding

There was no funding for this paper.

Disclosure

The authors declare that they have no competing interests.

References

1. Bray F, Ferlay J, Soerjomataram I, Siegel RL, Torre LA, Jemal A. Global cancer statistics 2018: GLOBOCAN estimates of incidence and mortality worldwide for 36 cancers in 185 countries. *CA Cancer J Clin*. 2018;68(6):394–424. doi:10.3322/caac.21492
2. Crosbie EJ, Kitson SJ, McAlpine JN, Mukhopadhyay A, Powell ME, Singh N. Endometrial cancer. *Lancet*. 2022;399(10333):1412–1428. doi:10.1016/s0140-6736(22)00323-3

3. Karpel HC, Chern JY, Smith JM, Smith AJ, Pothuri B. Utility of germline multi-gene panel testing in patients with endometrial cancer. *Gynecol Oncol*. 2022;165(3):546–551. doi:10.1016/j.ygyno.2022.04.003
4. Onstad MA, Schmandt RE, Lu KH. Addressing the role of obesity in endometrial cancer risk, prevention, and treatment. *J Clin Oncol*. 2016;34(35):4225–4230. doi:10.1200/jco.2016.69.4638
5. Colombo N, Creutzberg C, Amant F, et al. ESMO-ESGO-ESTRO Consensus Conference on Endometrial Cancer: diagnosis, treatment and follow-up. *Ann Oncol*. 2016;27(1):16–41. doi:10.1093/annonc/mdv484
6. Heudel P, Frenel JS, Dalban C, et al. Safety and efficacy of the mTOR inhibitor, vistusertib, combined with anastrozole in patients with hormone receptor-positive recurrent or metastatic endometrial cancer: the Victoria multicenter, open-label, phase 1/2 randomized clinical trial. *JAMA Oncol*. 2022;8(7):1001. doi:10.1001/jamaoncol.2022.1047
7. Horeweg N, Workel HH, Loiero D, et al. Tertiary lymphoid structures critical for prognosis in endometrial cancer patients. *Nat Commun*. 2022;13(1):1373. doi:10.1038/s41467-022-29040-x
8. Siegenthaler F, Lindemann K, Epstein E, et al. Time to first recurrence, pattern of recurrence, and survival after recurrence in endometrial cancer according to the molecular classification. *Gynecol Oncol*. 2022;165(2):230–238. doi:10.1016/j.ygyno.2022.02.024
9. Egawa-Takata T, Ueda Y, Ito K, et al. Adjuvant Chemotherapy for Endometrial Cancer (ACE) trial: a randomized Phase II study for advanced endometrial carcinoma. *Cancer Sci*. 2022;113(5):1693–1701. doi:10.1111/cas.15310
10. Liu D, Kaufmann GF, Breitmeyer JB, Dickson KA, Marsh DJ, Ford CE. The anti-ROR1 monoclonal antibody zilovetamab inhibits the proliferation of ovarian and endometrial cancer cells. *Pharmaceutics*. 2022;14(4):Apr. doi:10.3390/pharmaceutics14040837
11. Lheureux S, Matei DE, Konstantinopoulos PA, et al. Translational randomized phase II trial of cabozantinib in combination with nivolumab in advanced, recurrent, or metastatic endometrial cancer. *J Immunother Cancer*. 2022;10(3):e004233. doi:10.1136/jitc-2021-004233
12. Zheng J, Conrad M. The metabolic underpinnings of ferroptosis. *Cell Metab*. 2020;32(6):920–937. doi:10.1016/j.cmet.2020.10.011
13. Li J, Cao F, Yin HL, et al. Ferroptosis: past, present and future. *Cell Death Dis*. 2020;11(2):88. doi:10.1038/s41419-020-2298-2
14. Tang D, Chen X, Kang R, Kroemer G. Ferroptosis: molecular mechanisms and health implications. *Cell Res*. 2021;31(2):107–125. doi:10.1038/s41422-020-00441-1
15. Liang C, Zhang X, Yang M, Dong X. Recent progress in ferroptosis inducers for cancer therapy. *Adv Mater*. 2019;31(51):e1904197. doi:10.1002/adma.201904197
16. He J, Ding H, Li H, Pan Z, Chen Q. Intra-tumoral expression of SLC7A11 is associated with immune microenvironment, drug resistance, and prognosis in cancers: a pan-cancer analysis. *Front Genet*. 2021;12:770857. doi:10.3389/fgene.2021.770857
17. Koppula P, Zhuang L, Gan B. Cystine transporter SLC7A11/xCT in cancer: ferroptosis, nutrient dependency, and cancer therapy. *Protein Cell*. 2021;12(8):599–620. doi:10.1007/s13238-020-00789-5
18. Cheng X, Wang Y, Liu L, Lv C, Liu C, Xu J. SLC7A11, a potential therapeutic target through induced ferroptosis in colon adenocarcinoma. *Front Mol Biosci*. 2022;9:889688. doi:10.3389/fmolb.2022.889688
19. Guan Z, Chen J, Li X, Dong N. Tanshinone IIA induces ferroptosis in gastric cancer cells through p53-mediated SLC7A11 down-regulation. *Biosci Rep*. 2020;40(8):BSR20201807. doi:10.1042/bsr20201807
20. Huang W, Chen K, Lu Y, et al. ABCG5 facilitates the acquired resistance of sorafenib through the inhibition of SLC7A11-induced ferroptosis in hepatocellular carcinoma. *Neoplasia*. 2021;23(12):1227–1239. doi:10.1016/j.neo.2021.11.002
21. Zhang N, Huang J, Xu M, Wang Y. LncRNA T-UCR Uc.339/miR-339/SLC7A11 axis regulates the metastasis of ferroptosis-induced lung adenocarcinoma. *J Cancer*. 2022;13(6):1945–1957. doi:10.7150/jca.65017
22. Safran M, Dalah I, Alexander J, et al. GeneCards Version 3: the human gene integrator. *Database*. 2010;2010:baq020. doi:10.1093/database/baq020
23. Consortium U. UniProt: the universal protein knowledgebase in 2021. *Nucleic Acids Res*. 2021;49(D1):D480–d489. doi:10.1093/nar/gkaa1100
24. Liu W, Xie Y, Ma J, et al. IBS: an illustrator for the presentation and visualization of biological sequences. *Bioinformatics*. 2015;31(20):3359–3361. doi:10.1093/bioinformatics/btv362
25. Navarro Gonzalez J, Zweig AS, Speir ML, et al. The UCSC Genome Browser database: 2021 update. *Nucleic Acids Res*. 2021;49(D1):D1046–d1057. doi:10.1093/nar/gkaa1070
26. Thul PJ, Lindskog C. The human protein atlas: a spatial map of the human proteome. *Protein Sci*. 2018;27(1):233–244. doi:10.1002/pro.3307
27. Li T, Fu J, Zeng Z, et al. TIMER2.0 for analysis of tumor-infiltrating immune cells. *Nucleic Acids Res*. 2020;48(W1):W509–w514. doi:10.1093/nar/gkaa407
28. Tang Z, Kang B, Li C, Chen T, Zhang Z. GEPIA2: an enhanced web server for large-scale expression profiling and interactive analysis. *Nucleic Acids Res*. 2019;47(W1):W556–w560. doi:10.1093/nar/gkz430
29. Day RS, McDade KK. A decision theory paradigm for evaluating identifier mapping and filtering methods using data integration. *BMC Bioinform*. 2013;14:223. doi:10.1186/1471-2105-14-223
30. Lániczky A, Györfy B. Web-based survival analysis tool tailored for medical research (KMplot): development and implementation. *J Med Internet Res*. 2021;23(7):e27633. doi:10.2196/27633
31. Koch A, De Meyer T, Jeschke J, Van Criekinge W. MEXPRESS: visualizing expression, DNA methylation and clinical TCGA data. *BMC Genomics*. 2015;16(1):636. doi:10.1186/s12864-015-1847-z
32. Modhukur V, Iljasenko T, Metsalu T, Lokk K, Laisk-Podar T, Vilo J. MethSurv: a web tool to perform multivariable survival analysis using DNA methylation data. *Epigenomics*. 2018;10(3):277–288. doi:10.2217/epi-2017-0118
33. Ru B, Wong CN, Tong Y, et al. TISIDB: an integrated repository portal for tumor-immune system interactions. *Bioinformatics*. 2019;35(20):4200–4202. doi:10.1093/bioinformatics/btz210
34. Huang J, Chen Z, Ding C, Lin S, Wan D, Ren K. Prognostic biomarkers and immunotherapeutic targets among CXCL chemokines in pancreatic adenocarcinoma. *Front Oncol*. 2021;11:711402. doi:10.3389/fonc.2021.711402
35. Cramer DW. The epidemiology of endometrial and ovarian cancer. *Hematol Oncol Clin North Am*. 2012;26(1):1–12. doi:10.1016/j.hoc.2011.10.009
36. Siegel RL, Miller KD, Fuchs HE, Jemal A. Cancer Statistics, 2021. *CA Cancer J Clin*. 2021;71(1):7–33. doi:10.3322/caac.21654
37. Brooks RA, Fleming GF, Lastra RR, et al. Current recommendations and recent progress in endometrial cancer. *CA Cancer J Clin*. 2019;69(4):258–279. doi:10.3322/caac.21561
38. Li P, Brown S, Williams M, et al. The genetic landscape of germline DDX41 variants predisposing to myeloid neoplasms. *Blood*. 2022. doi:10.1182/blood.2021015135

39. Lin X, Xiao M, Chen Z, Ding C, Zhang T, Li Q. Pancancer analyses reveal genomics and clinical characteristics of the SETDB1 in human tumors. *J Oncol*. 2022;2022:6115878. doi:10.1155/2022/6115878
40. Saito Y, Koya J, Kataoka K. Multiple mutations within individual oncogenes. *Cancer Sci*. 2021;112(2):483–489. doi:10.1111/cas.14699
41. Cortés-Ciriano I, Lee JJ, Xi R, et al. Comprehensive analysis of chromothripsis in 2658 human cancers using whole-genome sequencing. *Nat Genet*. 2020;52(3):331–341. doi:10.1038/s41588-019-0576-7
42. Liu L, He J, Sun G, et al. The N6-methyladenosine modification enhances ferroptosis resistance through inhibiting SLC7A11 mRNA deadenylation in hepatoblastoma. *Clin Transl Med*. 2022;12(5):e778. doi:10.1002/ctm2.778
43. Yang WS, Stockwell BR. Ferroptosis: death by lipid peroxidation. *Trends Cell Biol*. 2016;26(3):165–176. doi:10.1016/j.tcb.2015.10.014
44. Guo J, Xu B, Han Q, et al. Ferroptosis: a novel anti-tumor action for cisplatin. *Cancer Res Treat*. 2018;50(2):445–460. doi:10.4143/crt.2016.572
45. Fang X, Cai Z, Wang H, et al. Loss of cardiac ferritin H facilitates cardiomyopathy via Slc7a11-mediated ferroptosis. *Circ Res*. 2020;127(4):486–501. doi:10.1161/circresaha.120.316509
46. Lang X, Green MD, Wang W, et al. Radiotherapy and immunotherapy promote tumoral lipid oxidation and ferroptosis via synergistic repression of SLC7A11. *Cancer Discov*. 2019;9(12):1673–1685. doi:10.1158/2159-8290.Cd-19-0338
47. Qian L, Wang F, Lu SM, et al. A comprehensive prognostic and immune analysis of ferroptosis-related genes identifies SLC7A11 as a novel prognostic biomarker in lung adenocarcinoma. *J Immunol Res*. 2022;2022:1951620. doi:10.1155/2022/1951620
48. Lin Y, Dong Y, Liu W, Fan X, Sun Y. Pan-cancer analyses confirmed the ferroptosis-related gene SLC7A11 as a prognostic biomarker for cancer. *Int J Gen Med*. 2022;15:2501–2513. doi:10.2147/ijgm.S341502
49. Liu R, Liu L, Bian Y, et al. The dual regulation effects of ESR1/NEDD4L on SLC7A11 in breast cancer under ionizing radiation. *Front Cell Dev Biol*. 2021;9:772380. doi:10.3389/fcell.2021.772380
50. Li Y, Zeng X, Lu D, Yin M, Shan M, Gao Y. Erastin induces ferroptosis via ferroportin-mediated iron accumulation in endometriosis. *Hum Reprod*. 2021;36(4):951–964. doi:10.1093/humrep/deaa363
51. Ng SW, Norwitz SG, Taylor HS, Norwitz ER. Endometriosis: the role of iron overload and ferroptosis. *Reprod Sci*. 2020;27(7):1383–1390. doi:10.1007/s43032-020-00164-z
52. Bielfeld AP, Pour SJ, Poschmann G, Stühler K, Krüssel JS, Baston-Büst DM. A proteome approach reveals differences between fertile women and patients with repeated implantation failure on endometrial level – does hCG render the endometrium of RIF patients? *Int J Mol Sci*. 2019;20(2):425. doi:10.3390/ijms20020425
53. Zhang M, Zhang T, Song C, et al. Guizhi Fuling Capsule ameliorates endometrial hyperplasia through promoting p62-Keap1-NRF2-mediated ferroptosis. *J Ethnopharmacol*. 2021;274:114064. doi:10.1016/j.jep.2021.114064
54. Tokunaga H, Shimada M, Ishikawa M, Yaegashi N. TNM classification of gynaecological malignant tumours, eighth edition: changes between the seventh and eighth editions. *Jpn J Clin Oncol*. 2019;49(4):311–320. doi:10.1093/jjco/hyy206
55. Chang MT, Asthana S, Gao SP, et al. Identifying recurrent mutations in cancer reveals widespread lineage diversity and mutational specificity. *Nat Biotechnol*. 2016;34(2):155–163. doi:10.1038/nbt.3391
56. Moore LD, Le T, Fan G. DNA methylation and its basic function. *Neuropsychopharmacology*. 2013;38(1):23–38. doi:10.1038/npp.2012.112
57. Sokratous G, Polyzoidis S, Ashkan K. Immune infiltration of tumor microenvironment following immunotherapy for glioblastoma multiforme. *Hum Vaccin Immunother*. 2017;13(11):2575–2582. doi:10.1080/21645515.2017.1303582
58. Braun DA, Hou Y, Bakouny Z, et al. Interplay of somatic alterations and immune infiltration modulates response to PD-1 blockade in advanced clear cell renal cell carcinoma. *Nat Med*. 2020;26(6):909–918. doi:10.1038/s41591-020-0839-y
59. Luo L, Li L, Liu L, et al. A necroptosis-related lncRNA-based signature to predict prognosis and probe molecular characteristics of stomach adenocarcinoma. *Front Genet*. 2022;13:833928. doi:10.3389/fgene.2022.833928
60. Lopez de Rodas M, Nagineni V, Ravi A, et al. Role of tumor infiltrating lymphocytes and spatial immune heterogeneity in sensitivity to PD-1 axis blockers in non-small cell lung cancer. *J Immunother Cancer*. 2022;10(6):e004440. doi:10.1136/jitc-2021-004440
61. Gao W, Wang X, Zhou Y, Wang X, Yu Y. Autophagy, ferroptosis, pyroptosis, and necroptosis in tumor immunotherapy. *Signal Transduct Target Ther*. 2022;7(1):196. doi:10.1038/s41392-022-01046-3
62. Ferrall L, Lin KY, Roden RBS, Hung C-F, Wu T-C. Cervical cancer immunotherapy: facts and hopes. *Clin Cancer Res*. 2021;27(18):4953–4973. doi:10.1158/1078-0432.Ccr-20-2833